Appl Phys B manuscript No.
(will be inserted by the editor)

Bose-Einstein Condensates in Magnetic Waveguides

J. Fortágh, H. Ott, S. Kraft, A. Günther, and C. Zimmermann

Physikalisches Institut der Universität Tübingen
Auf der Morgenstelle 14, 72076 Tübingen, Germany

Received: date / Revised version: date

Abstract In this article, we describe an experimental system for generating Bose-Einstein condensates and controlling the shape and motion of the condensate by using miniaturised magnetic potentials. In particular, we describe the magnetic trap setup, the vacuum system, the use of dispenser sources for loading a high number of atoms into the magneto-optical trap, the magnetic transfer of atoms into the microtrap, and the experimental cycle for generating Bose-Einstein condensates. We present first results on outcoupling of condensates into a magnetic waveguide and discuss influences of the trap surface on the ultracold ensembles.
PACS: 03.75.Fi, 03.75.Be, 34.50.Dy, 75.70.-i

1 Introduction

After seven years of research with Bose-Einstein condensates it was now possible to significantly simplify the complexity of the first generation experimental apparatus. In recent experiments condensates have been generated with a duty cycle of only a few seconds [1,2]. Furthermore, it was possible to avoid Zeeman slowing techniques [3] or complex combinations of two magneto-optical traps [4] by using a pulsed alkali dispenser source [5]. With these developements, it is now conceivable to construct a compact and portable apparatus for application oriented experiments with macroscopic atomic matter waves. A breakthrough in this direction has been achieved recently with the successful loading of magnetic microtraps [6,2] with Bose-Einstein condensates. In principal, magnetic microtraps allow for the construction of a large variety of trapping potentials. Thus, a growing number of research groups start to explore the possibilities which arise from the combination of micropotentials with degenerate atomic quantum gases [7,8,9]. Here, we describe in some detail our experimental approach including the apparatus that we use to load a condensate into a magnetic microtrap. First experimental results on outcoupling a condensate from a trap into the waveguide are presented. We comment recent measurements of the lifetime, heating rate and fragmentation of ultracold atomic clouds close to a conductor surface [10]. We conclude the article with speculations about future developments to atom optics on a microchip.

2 Experimental setup

For studies on ultracold quantum gases in elongated waveguides, we have developed a method for loading a large number of atoms into tightly confining traps at a microstructure. The key feature is the continuous transformation of a rather shallow magnetic potential into the tightly confining geometry of the microtrap [11,12]. The atoms are initially collected in a magneto-optical trap (MOT) and subsequently loaded into the shallow magnetic quadrupole trap employing standard techniques of polarisation gradient cooling and optical pumping. Afterwards, the atoms are adiabatically compressed into the microtrap by gradually transforming the magnetic field. The compression enhances the collision rate and accelerates the thermalisation. When the collision rate is several 10 per second the atomic gas can be efficiently cooled by forced evaporation into the degenerate regime.

The trap setup employed in our experiments is shown in Fig. 1. The microtrap is arranged between the 'transfer coils'. For the operation of the MOT we use a second pair of coils: the 'MOT-coils'. The MOT is working in a six beam configuration with beam diameters of 20 mm and 20 mW of laser power in each beam. The separation of the MOT-coils and transfer coils guaranties an undisturbed operation of the MOT and allows for high flexibility in mounting different microtrap geometries. Thus, different microtraps can be loaded by the same transfer scheme. The microstructure with microfabricated current conductors is mounted horizontally upside down below the 'compression wire', and the magnetic microtrap is generated below the microstructure. The

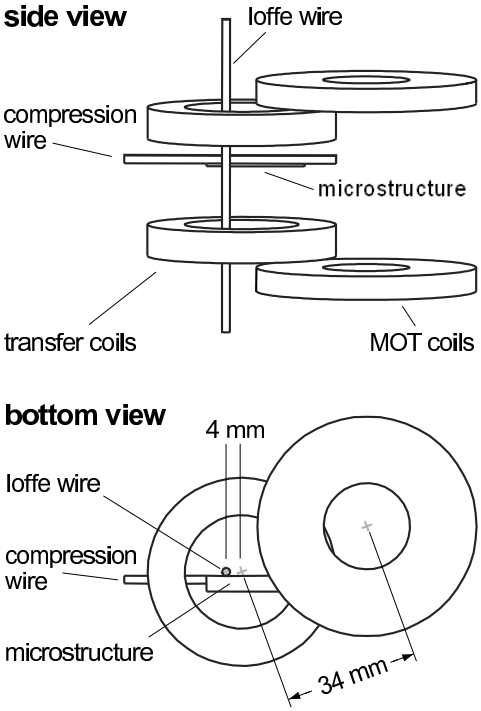

Fig. 1 Trap setup. The magnetic trap setup consists of two pair of coils, a Ioffe-wire, a compression wire, a microstructure with microsized conductors, and a thin copper wire parallel to the microstructure. The MOT is generated at the right hand side between the MOT-coils. The magnetic microtrap is arranged between the transfer coils. The MOT-coils have an inner diameter of 22 mm and 130 windings on each coil. The distance between the MOT-coils is 48 mm. The transfer coils have an inner diameter of 31 mm and 80 windings on each coil. The vertical distance between the transfer coils is 30 mm. The MOT-coils and transfer coils are separated by 34 mm. The Ioffe-wire has a diameter of 2 mm and a circular cross section. It is displaced by 4 mm to the symmetry axis of the transfer coils. The compression wire has a quadratic cross section with a width of 2 mm. It is placed horizontally 4 mm above the symmetry plane of the coils and the centre of the Ioffe-trap [13]. The surface of the microstructure has a distance of 2.2 mm to the central plane of the coils. The compression wire, the microstructure and the thin copper wire are mounted on a heat sink between the transfer coils. The photograph shows the mounted trap setup and the dispenser sources behind the MOT-coils.

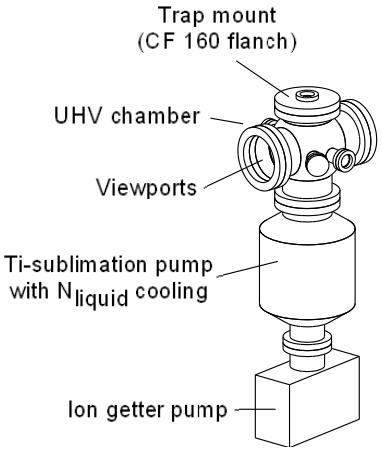

Fig. 2 The vacuum system. The vacuum chamber is pumped by a titanium sublimation pump with liquid nitrogen cooling and an ion getter pump to achieve UHV conditions with a base pressure of 1×10^{-11} mbar. The trap setup shown in Fig.1 is mounted at the cover of the vacuum chamber.

Ioffe-geometry of the magnetic traps between the transfer coils is provided by combining the magnetic fields of the transfer coils and an additional vertical wire: the 'Ioffe-wire' [13]. The Ioffe-wire passes the transfer coils parallel to their symmetry axis with a lateral displacement of 4 mm. The Ioffe-trap is built in the middle of a semi circular trajectory which connects the centre of the quadrupole field of the transfer coils and the middle of the Ioffe-wire [13]. This trap can be shifted in its vertical position by varying the currents in the transfer coils. For the transfer into the microtrap, it is necessary that the compression wire and at least one of the microfabricated conductors are oriented parallel to the long axis of the Ioffe-trap and that they are aligned in the plane in which the Ioffe-trap can be shifted up and down.

The trap setup is placed in a vacuum chamber at a base pressure of 1×10^{-11} mbar. Ultrahigh vacuum conditions are achieved in a system shown in Fig. 2. The vacuum chamber is pumped by an ion getter pump (80 l/s) and a titanium sublimation pump (2500 l/s) cooled by liquid nitrogen. The configuration of electromagnets and the dispenser sources are mounted at the cover of the vacuum chamber. View ports with antireflexion coating at the side and top of the chamber ensure good optical access to the inside and allow the operation of a six-beam magneto-optical trap. The *in-vacuo* setup is built by UHV compatible components using OFHC-copper, stainless steel, MACOR, Al_2O_3-ceramics, ceramic glue, and capton insulated copper wires. The dissipated heat during the operation of the microelectromagnets, especially the heat generated by the transfer coils of about 9 W, by the compression wire and Ioffe-wire of 2 W each and the microsized conductors of up to 10 W, is conducted by a copper rod to a liquid nitrogen reservoir outside the chamber. It ensures a constant temperature for the microstructure at approximately $-15°$C which

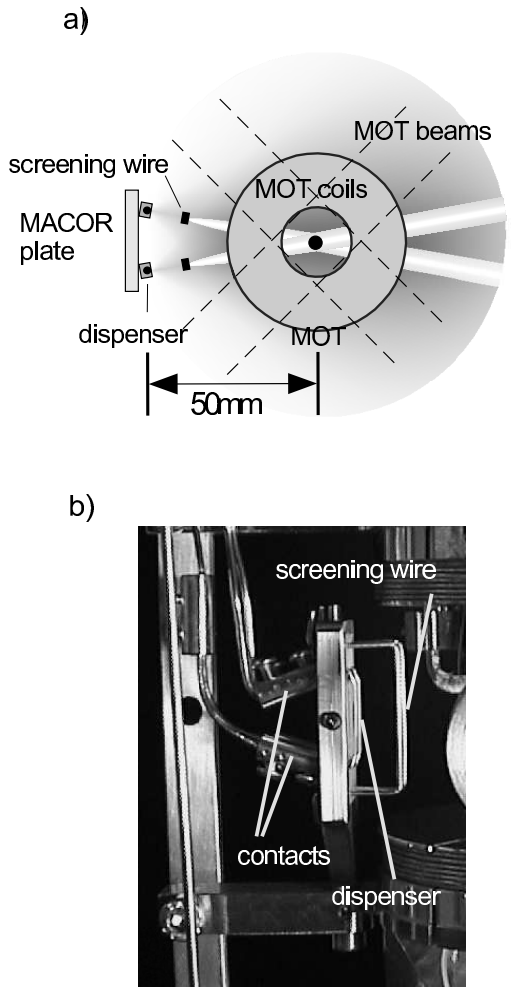

Fig. 3 The dispenser sources for thermal rubidium atoms. (a) top view: The MOT is loaded by a pair of dispensers which emit a beam of rubidium atoms towards the trapping region of the MOT. The screening wires prevent a direct impact of the beam to the centre of the MOT. (b) The dispenser mount (side view). The ends of the dispensers are fed through a MACOR plate. At the back side, they are fixed to the supplying copper conductors.

was determined from the measured resistance of the copper conductors. Without cooling, the trap setup warms up, and the lifetime of the atomic clouds is shortened, nevertheless it can still be used for experiments with Bose-Einstein condensates.

As source for thermal rubidium atoms we use a pair of resistively heated dispensers [5]. The dispensers are located at a distance of 50 mm from the MOT (Fig. 3). They are mounted in a MACOR ceramic plate as shown in Fig. 3b. The ends of the dispensers are bent back at 90 degree and pass through holes in the plate. They are mechanically fixed behind the plate to the copper conductors supplying power. The bending allows for flexing and thermal expansion of the heated metal container. The dispensers are heated by currents of opposite directions to each other. Because of this symmetrical con-

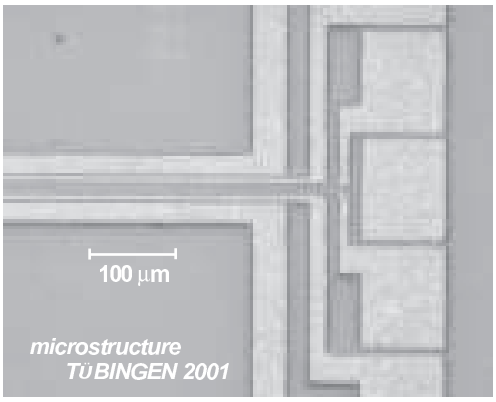

Fig. 4 The microstructure consists of seven parallel copper conductors with a width of 30, 11, 3, 3, 3, 11, and 30 μm and a height of 2.5 μm. On the right hand side the contact pads are visible (microscope image).

figuration it is possible to avoid a shifting of the MOT position due to the magnetic field of the current flow in the nearby dispensers. If the dispensers are heated by a current of a few amps a thermal rubidium beam is emitted into the trapping region of the MOT (Fig. 3a). A screening wire with 1 mm diameter in front of the rubidium source shields the centre of the MOT and prevents the magneto-optically trapped atoms from direct impact of thermal atoms and other contaminations from the heated area. Without screening, the lifetime of the MOT is strongly reduced due to fast decay processes on a time scale of a few seconds. The screening eliminates the losses and a smooth decay behaviour of the MOT due to the background pressure can be observed.

3 The Microstructure

For the current investigations on ultracold atomic gases, the magnetic trap is built at a microstructure consisting of seven 22 mm long parallel copper conductors. The microfabricated conductors are electroplated on an Al_2O_3 substrate (Fig. 4) and have widths of 30, 11, 3, 3, 3, 11, and 30 μm, respectively. Their nominal separation is 1 μm and the height of the electroplated copper layer is 2.5 μm [14]. The microstructure is mounted onto the surface of the compression wire, with theconductors oriented parallel to the compression wire. For reference measurements, a thin copper wire with a diameter of 90 μm and a length of 25 mm is mounted parallel to the microstructure. It can be used alternatively to the conductors at the microstructure for generating a linear microtrap [10]. The vertical distance between the middle of the compression wire and the microfabricated conductors is 1.8 mm and the distance between the middle of the compression wire and the thin wire is 2.0 mm.

The combination of linear conductors and a bias field perpendicular to the axis of the conductor enables a large variety of radial trap geometries to be built. In the sim-

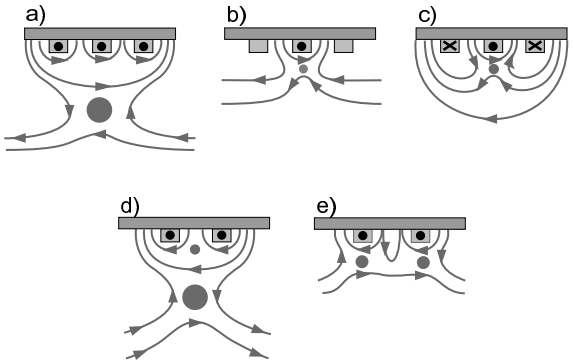

Fig. 5 Waveguide geometries at current carrying linear coductors. The orientation of the driving current is marked by • and ×. The arrows show schematically the slope of the magnetic field. The filled circles indicates the trap centres. a) and b) show waveguide geometries formed by the microstructure and an additional external bias field. In c) the bias field is generated by the outer conductors of the microstructure. d) and e) show multiple waveguide configurations. Depending on the strength of the bias field, the two waveguides are located side by side or on top of each other.

plest case, several conductors are driven with currents in the same direction and the trap is generated by applying an additional bias field perpendicular to the conductors (Fig. 5a). An additional axial offset field provides the parabolic potential shape in the centre of the waveguide. Turning off the outer conductors shifts the position of the trap closer to the inner conductor (Fig. 5b) and increases the radial gradient. The depth of the magnetic trap is determined by the bias field applied perpendicular to the conductors and does not change during the compression. The trap can be further compressed by inverting the currents in the neighbouring conductors (Fig. 5c). Calculations with the measured maximum current densities in the microconductors [14] predict a maximal possible radial oscillation frequency of $2\pi \times 600\,000\,\mathrm{Hz}$. Starting with standard trap parameters for Bose-Einstein condensation ($\omega_\mathrm{r} = 2\pi \times 300\,\mathrm{Hz}$ and $\omega_\mathrm{a} = 2\pi \times 14\,\mathrm{Hz}$ radial and axial oscillation frequencies, respectively), it should be possible to change the aspect ratio of the trap about three orders of magnitude. A further application of parallel current conductors is the construction of parallel waveguides [15]. The waveguides can be arranged horizontally or vertically to each other depending on the strength of the applied bias field (Fig. 5d and 5e). If the bias field is oriented exactly parallel to the plane defined by the conductors, the trajectories of the trap centres cross each other while changing the bias field and the waveguides can be merged and separated.

4 Experimental cycle

At the begining of the experiment the MOT is loaded within 25 s from pulsed thermal dispenser sources. Thereby, 3×10^8 ^{87}Rb atoms are collected at a temperature of

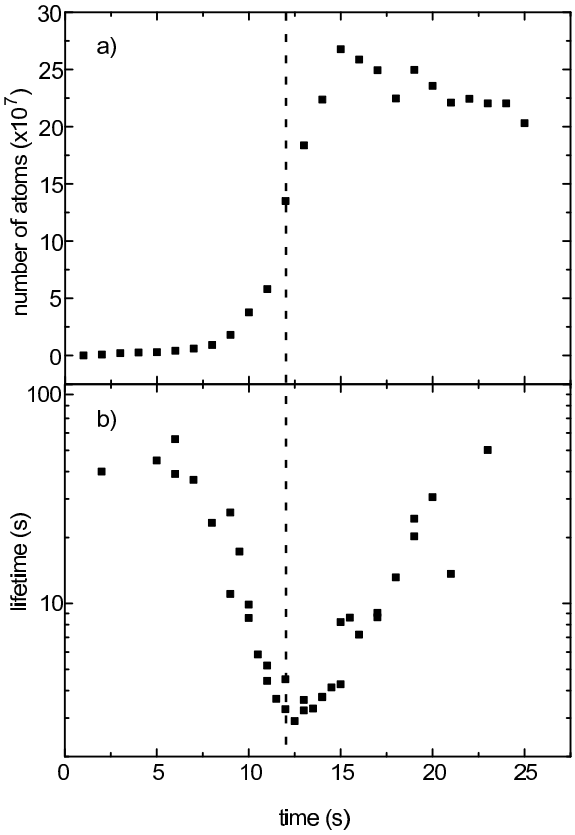

Fig. 6 Loading the MOT from the pulsed dispenser sources. a) Time evolution of the number of atoms in the MOT. b) Time evolution of the lifetime of trapped atomic clouds between the MOT-coils during the loading process. The heating current (6.5A) of the dispenser is turned on at the starting point of the diagram and it is turned off after 12 s (dashed line). After switching off the dispenser current, the lifetime recovers in approximately 10 s after them the atoms are restored into the magnetic trap.

$50\,\mu$K. During the first 12 seconds, the dispensers are heated by a constant current pulse of 6.5 A. For the next 13 seconds, the dispensers are turned off and the MOT is loaded from the thermal rubidium beam and the residual vapour. The time evolution of the number of atoms and their lifetime is shown in Fig. 6. Approximately seven seconds after switching on the heating current, the dispensers reach the dissociation temperature of rubidium and the emission starts. The local pressure of rubidium grows and the MOT is loaded on a time scale within its lifetime. After switching off the heating, the dispensers rapidly cool down below the dissociation temperature, predominantly due to thermal radiation [5]. Within the next few seconds, the rubidium vapour is pumped out and the initial trap lifetime of about 60 s is recovered. The data points in Fig. 6a and Fig. 6b have been measured in separate experimental cycles. The number of atoms was detected by absorption imaging.

The preparation of ultracold atoms in the MOT is finished by 10 ms polarisation gradient cooling. Then, the atoms are optically pumped into the $|\mathrm{F}=2, \mathrm{m_F}=$

$2>$ hyperfine ground state and a $60\,\mu$K cold cloud of 2×10^8 atoms is loaded into the spherical quadrupole trap formed by the MOT-coils at a field gradient of 45 G/cm. Because the MOT-coils and the transfer coils overlap, an adiabatic transfer of the magnetically trapped atoms can be performed: the quadrupole potential minimum moves on a straight line from the centre of the MOT-coils to the centre of the transfer coils. At a current of 3 A the transfer coils generate a spherical quadrupole field with a gradient of 58 G/cm along the symmetry axis. By increasing the current in the Ioffe-wire, the centre of the spherical quadrupole is shifted and transformed into a Ioffe-type trapping field [13]. At a current of 13 A in the Ioffe-wire the resulting harmonic trap potential is characterised by its axial oscillation frequency of $\omega_\mathrm{a} = 2\pi\times14\,\mathrm{Hz}$, its radial oscillation frequency of $\omega_\mathrm{r} = 2\pi\times110\,\mathrm{Hz}$, and the offset field of 0.4 G in the middle of the trap. In this Ioffe-type trap the atoms are cooled for 20 s by radio frequency evaporation to a temperature of $5\,\mu$K. In this large volume Ioffe-trap, condensation can be reached with approximately 2×10^4 atoms if the cloud is cooled for a further 10 s. However, the transfer into the microtrap offers more advantageous conditions for condensation.

Therefore, after 20 s of precooling in the large volume Ioffe-trap, the ensemble is compressed adiabatically into the microtrap by reducing the current in the upper transfer coil. This shifts the trap minimum to the microstructure (Fig. 7). For a tighter confinement of the cloud in the microtrap, a current in the compression wire can be applied. Good conditions for Bose-Einstein condensation have been achieved for a large range of radial oscillation frequencies between $\omega_\mathrm{r} = 2\pi\times200\,\mathrm{Hz}$ and $2\pi\times2\,000\,\mathrm{Hz}$. The axial confinement is determined by the Ioffe-trap to $\omega_\mathrm{a} = 2\pi\times14\,\mathrm{Hz}$ in all experiments. The compression from the Ioffe-trap into the microtrap takes place within 1 s and is completed by applying the current in the compression wire. During the transfer and compression the radio frequency is turned off. The compression heats the atomic cloud by a factor of up to 7 and boosts the elastic collision rate to several hundred per second. By now ramping down the radio frequency from 5 MHz to about 1 MHz within 5 s we reach condensation with up to 1×10^6 atoms at a critical temperature of typically between 500 nK and $1\,\mu$K [6].

The radial confinement of an elongated trap is determined in principal by the current in the microconductor and the compression wire [10]. However, additional bias fields from the Ioffe-wire and the transfer coils can significantly modify this value. Therefore, we measure the exact trap frequencies by sinusoidal perturbating the trapping potential and observing the temperature of the thermal cloud. To complete the characterisation of the trap, we measure the bias field in the centre of the trap by removing all the atoms via rf-outcoupling.

The parameters of the Bose-Einstein condensate such as the number of atoms, the chemical potential and the density are derived from absorption images after several milliseconds time of flight. Condensates in tightly confining traps are generated at high densities of about $10^{15}\,\mathrm{cm}^{-3}$. Due to inelastic three body losses [16] the lifetime is in the order of a hundred millisecond. By reducing the density, the lifetime of the condensate can be enhanced up to several seconds in which subsequent investigations on the Bose-Einstein condensate can be performed [10]. Thereby, magnetic microtraps allow a fast and versatile manipulation of the quantum gas. Altogether, the experimental cycle requires approximately one minute.

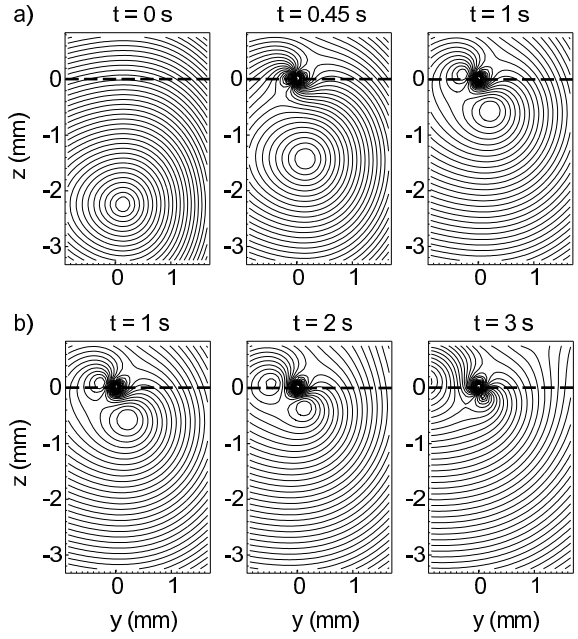

Fig. 7 Magnetic field contour plots (contour spacing 0.5 G) in the plane perpendicular to the microsized conductor located at y=0, z=0. The dashed line indicates the position of the microstructure's surface. The large volume Ioffe-trap is located at y=0, z=-2.2, its long axis is perpendicular to the illustrated plane. a) Transfer from the large volume Ioffe-trap into the microtrap within 1 s. The current in the microconductor (0.4 A) is switched on and the Ioffe-trap is shifted up by lowering the current in the upper transfer coil from 3 A to 2.3 A. The lower transfer coil carries a current of 3 A, the Ioffe-wire 13 A. As a result, the trap shifts up by approximately 1.6 mm and ends at a vertical displacement of $600\,\mu$m to the microsized conductor. b) Compression of the microtrap within 2 s. The current in the compression wire is increased to 2.7 A while simultaneously lowering the current in the upper transfer coil to 2 A. Reducing the current in the transfer coil is needed to avoid the saddle point moving into the microtrap. After the shown compression, the trap is located at a vertical distance of $200\,\mu$m to the middle of the microconductor.

5 Experiments

In applications on microtraps, the propagation of condensates in waveguides is of particular interest. An atomic

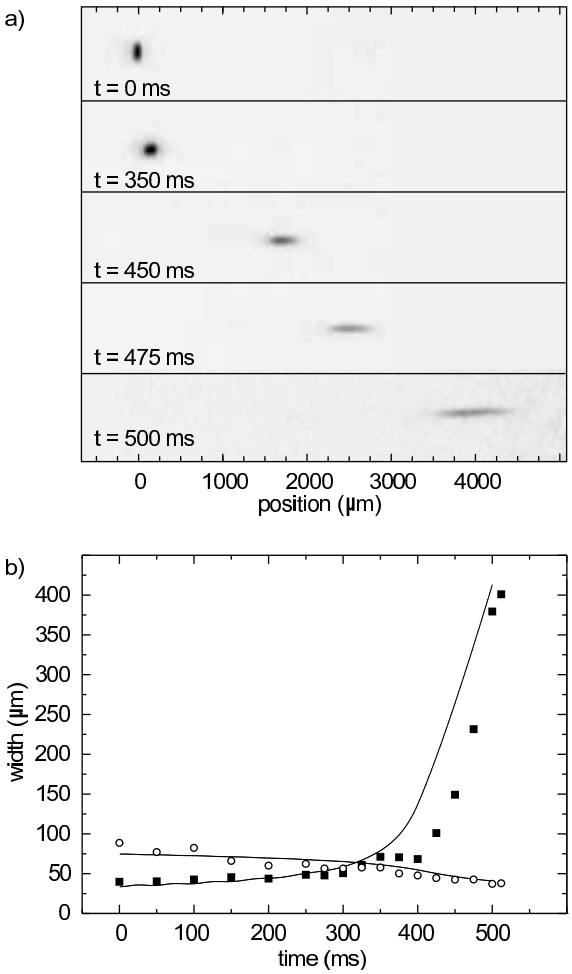

Fig. 8 Expansion of a condensate into the waveguide. The axial confinement of the magnetic trap is turned off within 400 ms and a gradient field forces the condensate into the waveguide. The release of the condensate into the waveguide is completed after 385 ms. (a) Position of the condensate at different stages of the expansion, after 23 ms time of flight (absorption images). The initial trap is located at the origin. (b) Time evolution of the radial (open circles) and the axial (filled squares) size of the condensate during the expansion. The straight lines show a numerical simulation of the time evolution of the condensate (see text).

beam could be guided from an on-chip atom laser to an experimental facility. For this reason an understanding of the outcoupling process from a trap into a waveguide and the physical properties of propagating condensates is required. We have started to study experimental scenarios where the condensate is released into a waveguide. Beginning with a condensate in a trap, characterized by the radial and axial oscillation frequencies of $\omega_{\rm r} = 2\pi \times 500\,{\rm Hz}$ and $\omega_a = 2\pi \times 14\,{\rm Hz}$, respectively, the axial confinement was turned off linearly within 0.4 s. An additional gradient field was turned on parallel to the guide axis which forces the condensate into the waveguide. In Fig. 8a five steps of the process are shown: the first image shows the condensate released from the initial trap after 23 ms time of flight. The condensate expands mostly in radial direction according to the tight confinement and high interaction energy. 0.35 s later, the axial confinement is already strongly reduced and the smaller radial size of the expanded condensate in the time of flight image indicates a decreased interaction energie. After 0.35 s the axial opening of the trap is no longer adiabatic due to the extreme low axial trap frequencies. 15 ms before the axial confinement is completely turned off, the condensate is released from the initial trap ($t = 385\,{\rm ms}$). The third image shows the condensate after 65 ms of propagation in the waveguide. The condensate still expands axially. Due to the external gradient field, it is accelerated by $0.38\,{\rm m/s^2}$. After 125 ms of propagation, it reaches a velocity of 48 mm/s. Fig. 8b shows the evolution of the expanded radial and axial width of the condensate after 23 ms time of flight during the expansion process. The radial width of the condensate decreases as the axial expansion lowers the density and the chemical potential. The straight lines in Fig. 8b are a numerical simulation of the radial and axial halflenghts of the condensate. The simulation is based on the scaling equations for a condensate in a time-dependent harmonic trap [17,18]. The trap was assumed to be at rest, while the axial curvature was linearly ramped down within 0.4 s. The centre of mass motion is decoupled from the inner excitations of the condensate which are well described by the theory. Note, that there is no fitting parameter in the theory. In future experiments, a detailed study of dynamics and coherence properties of elongated condensates and propagating beams may become feasible.

In recent experiments, the heating rate and the lifetime have been investigated on atomic clouds at small distances ($20 - 300\,\mu$m) to the surface of the microtrap [10]. It has been shown that the heating rate remains at each distances below 400 nK/s whereas the lifetime experience a reduction when approaching the surface. At a distance of $200\,\mu$m we measured a lifetime of 13 s which is reduced almost linearly to 2 s when the distance was reduced to $30\,\mu$m. However, the most peculiar effect which appears if atoms are moved into traps close to the surface of the conductor, is a fragmentation of the cloud along the conductor [10]. The fragmentation can be observed on ultracold and on condensed clouds. We have made the observations at the thin copper wire as well as along each microfabricated conductor. Fig. 9 shows the fragmentation of an expanding atomic cloud in a waveguide. These experiments indicate the general appearance of a periodic potential structure along current carrying copper conductors. The most probable structuring potential type is a magnetic one. Because an explanation of having a periodic structure of ferromagnetic contaminations on the conductors of different origin seems to be unlikely, we speculate whether the modulation corresponds to spin arrangements of moving electrons, a topic which is investigated be the research field of spintronics

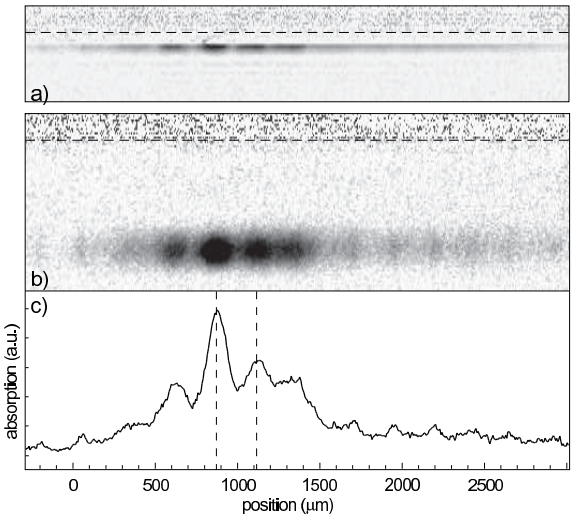

Fig. 9 The spatial density modulation of an expanding atomic cloud in the waveguide indicates a periodic potential structure along the current carrying copper conductor. For the experiment, an ultracold cloud of 5.6×10^5 atoms at the temperature of $1\,\mu$K was released into the waveguide by turning off the axial confinement of the trap within 400 ms. The waveguide had a radial confinement of $\omega_{\rm r} = 2\pi \times 1000\,$Hz. The absorption images were taken a) in the waveguide and b) after 10 ms time of flight. c) The integrated scan shows a periodicity of $260\,\mu$m in the density distribution of the cloud.

[19]. Meanwhile, the observations discussed above could be reproduced by two other groups [7,9] working on microtraps with copper conductors.

6 Outlook

Trapping and manipulating atoms in magnetic microtraps is a very young field and it is difficult to make predictions about future developments. Nevertheless, one can speculate about future research topics. The experiments presented in [10] show a strong influence of a nearby surface on a condensate. This suggests the use of the condensate as a probe to study an arbitrary surface. The sample surface can be either metallic or dielectric or a combination of both. Electric or magnetic surface forces, acting on the condensate will structure its density distribution. This can be observed with a variety of well established imaging techniques. In this case the resolution is limited by the imaging system to the micron range. A better resolution may be achieved by imaging the condensate after some milliseconds of free expansion in the gravitational field. Since such 'time of flight images' reflect the initial velocity distribution of the condensates, they would provide information about the phase gradients inside the condensate as imprinted by the surface under investigation. Such an approach can be regarded as an extension of recent experiments with condensates in three dimensional optical lattices [20]. By adiabatically reducing the lattice potential followed by a ballistic expansion, it was possible to directly image the population of the energy bands within the first Brillouin-zone. The size of the Brillouin-zone increases with decreasing lattice constant which means that the size of the time of flight images increases with decreasing size of the periodic structure. The limited resolution of the imaging system can be overcome in this way. By decomposing an arbitrary surface potential into periodic Fourier components one may be able to develop a novel kind of holographic surface microscope. These experiments can readily be done in a conventional Bose-Einstein apparatus by mounting a sample surface close to the centre of the magnetic trap and shifting the condensate towards the surface by varying the magnetic field of the trap in an appropriate way.

Another fascinating topic for future research with microtraps is the development of elements for integrated atom optical devices. If condensates can be split and recombined with temporal or spatial beam splitters it is conceivable to construct interferometers that are sensitive to rotations and forces [21]. Micropotentials can also be used to control the relative position between different atomic clouds or even single atoms. This allows for a tunable interaction between atoms and can be used for novel approaches to construct quantum gates[22].

In general, it appears that the generic dynamical process in magnetic micro potentials would be an oscillation rather than a current as in electronic circuits. Functional units may thus be envisioned as being constructed from oscillations that are conditionally coupled via their phase or amplitude. Quantum computers and other 'atom chip' devices may turn out to be a sophisticated combination of such 'computons'. In our experiment we have observed centre of mass oscillations of condensates with a very large quality factor. After suddenly shifting the minimum of the trapping potential that contains a condensate the resulting sloshing mode can be observed for several seconds. Its frequency of 7.9 Hz is determined with an relative error of 7×10^{-4} by fitting the data to a sine function. Although half of the atoms are lost during the experiment the oscillation amplitude is undamped within the uncertainty of the measurement and we estimate the quality factor of the oscillation to be better than 10 000. Magnetic microtrap potentials can be shaped in almost arbitrary ways such that nonlinear oscillations can be easily studied. In such potentials the centre of mass motion is coupled to collective excitations of the condensate and provides a periodic drive for the condensate shape oscillation. For the future it will certainly be interesting to investigate the dynamics of such a nonlinear system and study its suitability for the construction of atomic devices.

7 Acknowledgements

We thank G. Schlotterbeck, B. Herzog, and D. Wharam for the production of the microstructure, G. Ritt

and M. Ruder for the imaging software, S. Günther and C. Silber for numerical calculations, L. Borda for calculations on 1D systems, and G. Mihaly for discussions about spintronics. This work was supported in part by the Deutsche Forschungsgemeinschaft under Grant No. Zi 419/3.

References

1. M. D. Barrett, J.A. Sauer, and M.S. Chapman, Phys. Rev. Lett. **87,** 010404 (2001)
2. W. Hänsel, P. Hommelhoff, T.W. Hänsch, and J. Reichel, Nature **413,** 498 (2001)
3. J. Prodan, A. Migdall, W. D. Phillips, I. So, H. Metcalf, and J. Dalibard, Phys. Rev. Lett. **54,** 992 (1985)
4. C. J. Myatt, N. R. Newbury, R. W. Ghrist, S. Loutzenhiser, and C. E. Wieman, Opt. Lett. **21,** 290 (1996)
5. J. Fortagh, A. Grossmann, T.W. Hänsch, and C. Zimmermann, J. Appl. Phys. **84,** 6499 (1998)
6. H. Ott, J. Fortagh, G. Schlotterbeck, A. Grossmann, and C. Zimmermann, Phys. Rev. Lett. **87,** 230401 (2001)
7. A. E. Leanhardt, A. P. Chikkatur, D. Kielpinski, Y. Shin, T. L. Gustavson, W. Ketterle, and D. E. Pritchard, Phys. Rev. Lett. **89,** 040401 (2002)
8. A. Kasper, S. Scheider, C. v. Hagen, L. Feenstre, J. Schmiedmayer, 18th International Conference on Atomic Physics, Boston (2002)
9. M. P. A. Jones, C. J. Vale, K. Furusawa, E.A. Hinds, 18th International Conference on Atomic Physics, Boston (2002)
10. J. Fortagh, H. Ott, S. Kraft, and C. Zimmermann, cond-mat/0205310 (2002)
11. V. Vuletic, T. Fischer, M. Praeger, T. W. Hänsch, and C. Zimmermann, Phys. Rev. Lett. **80,** 1634 (1998)
12. J. Fortagh, A. Grossmann, C. Zimmermann, and T. W. Hänsch Phys. Rev. Lett. **81,** 5310 (1998)
13. J. Fortagh, H. Ott, A. Grossmann, and C. Zimmermann, Appl. Phys. B **70,** 701 (2000)
14. J. Fortagh, H. Ott, G. Schlotterbeck, C. Zimmermann, B. Herzog, and D. Wharam, Apl. Phys. Lett. **81,** 1146 (2002)
15. E. A. Hinds, C. J. Vale, and M. G. Boshier, Phys. Rev. Lett. **86,** 1462 (2001)
16. E. A. Burt, R. W. Ghrist, C. J. Myatt, M. J. Holland, E. A. Cornell, and C. E. Wieman, Phys. Rev. Lett. **79,** 337 (1997)
17. Y. Castin and R. Dum, Phys. Rev. Lett. **77,** 5315 (1996)
18. Yu. Kagan, E. L. Surkov, and G. V. Shlyapnikov, Phys. Rev. A **55,** R18 (1997)
19. S. Das Sarma, J. Fabian, X. Hu, I. Žutić, cond-mat/9912040 (2000)
20. M. Greiner, I. Bloch, O. Mandel, T. W. Hänsch, and T. Esslinger, Phys. Rev. Lett. **87,** 160405 (2001)
21. J. Reichel, W. Hänsel, P. Hommelhoff, and T. W. Hänsch, Appl. Phys. B **72,** 81 (2001), R. Folman, P. Krüger, J. Schmiedmayer, J. Denschlag, and C. Henkel, to appear in Adv. Opt. Mol. Phys. Vol 48 (Academic, New York 2002)
22. D. Jaksch, H.-J. Briegel, J. I. Cirac, C. W. Gardiner, and P. Zoller, Phys. Rev. Lett. **82,** 1975 (1999)